USS-Water Dataset and U-Net+ Model: A Novel High-Resolution Satellite Imagery Approach for Surface Water Detection in the United States

Nischal Vooda[1], Mohammed Sohaib Uddin[2], Abdul Rahman Shaikh[1], Mani Sai Lakshmi Karasani[1], M. Courtney Hughes[3], Mahdi Vaezi[4],*

[1]*College of Liberal Arts and Sciences, Department of Computer Science, Northern Illinois University, Dekalb, IL*

[2]*College of Business, Department of Operations Management and Information Systems, Northern Illinois University, Dekalb, IL*

[3]*College of Health and Human Sciences, School of Health Studies, Northern Illinois University, Dekalb, IL*

[4]*College of Engineering and Engineering Technology, Department of Engineering Technology, Northern Illinois University, Dekalb, IL*

Abstract

Water bodies are crucial for ecological balance and human development, necessitating accurate detection and monitoring. This paper introduces the USS-Water dataset and the U-Net+ model, an advanced approach for high-resolution satellite imagery-based surface water detection across the United States. The USS-Water dataset comprises 1,483 high-quality RGB satellite images from Google Earth, encompassing diverse water bodies such as rivers, lakes, oceans, and shipyards across 44 states. Each image features a resolution of 1,000×1,000 pixels and a high spatial resolution of 0.3 meters per pixel. The U-Net+ model, an enhancement of the traditional U-Net architecture, incorporates new layers and optimization techniques to improve segmentation accuracy and reduce computational complexity. This model addresses the high computational demands and inefficiencies of existing methods, particularly in processing large-scale, high-resolution satellite images. By optimizing for speed and accuracy, U-Net+ is tailored for real-time applications and can efficiently handle large datasets, making it a practical tool for widespread use. It is designed to work seamlessly with freely available RGB satellite images, offering a cost-effective solution for researchers, government agencies, policymakers, and NGOs involved in water resource management, environmental conservation, and disaster response. Comparative evaluation with DeepLabV3+ and MSResNet models demonstrates that U-Net+ achieves an Intersection over Union (IoU) score of 83.2%, precision of 0.98, recall of 0.88, and an F1-score of 93.6%. Case studies in downtown Chicago, IL, and Gary, IN, highlight the model's effectiveness in real-world scenarios, accurately predicting and delineating complex water bodies. The dataset and model are accessible for further research and practical applications, fostering advancements in surface water detection and monitoring.

1. Introduction

Water is a vital element for all life on Earth. Water bodies cover 71% of our planet's surface and play a crucial role in supporting biodiversity, ecological balance, and the growth of human societies (Vörösmarty et al. 2010). Using advanced satellite imagery is the most effective method for detecting and mapping surface water bodies, including ocean coastlines, reservoirs, wetlands, bays, shipyards, channels and canals, oases, hot springs, rivers, ponds, lakes, swamps, creeks,

straits, and lagoons. There are satellite imagery-based applications in water resources protection planning (Verma et al. 2021), mapping floods (Mateo-Garcia et al. 2021; Wieland et al. 2023), tracking changes in surface water (Cooley et al. 2017; Donchyts et al. 2016; C. Huang et al. 2018; Pekel et al. 2016), and water resources management/monitoring (Coskun, Gulergun, and Yilmaz 2006; Sawaya et al. 2003; Sheffield et al. 2018). Satellite imagery has emerged as a leading option for remote sensing compared to alternatives such as aerial photography (Sibanda et al. 2021), satellite- and ground-based sensors (Perumal, Sulaiman, and Leong 2015)(C. Huang et al. 2018), LiDAR (Light Detection and Ranging) (Q. Wu et al. 2019), and Synthetic Aperture Radar (SAR) (Behnamian et al. 2017; Vickers, Malnes, and Høgda 2019). Satellite imagery has surpassed aerial platforms in several key aspects, including wide coverage, regular monitoring (Becker-Reshef et al. 2010), cost-effectiveness (Wulder et al. 2012), remote accessibility (Xie, Sha, and Yu 2008), consistent calibration (Markham and Helder 2012), multi-spectral imaging (Goward et al. 2001), and rapid deployment (Justice et al. 2002).

Non-deep learning algorithms such as Normalized Difference Water Index (NDWI) (McFEETERS 1996), Modified Normalized Difference Water Index (MNDWI) (Xu 2006), High-Resolution Water Index (HRWI) (Yao et al. 2015), and Two-step Urban Water Index (TSUWI) (W. Wu et al. 2018) rely on spectral information for detecting surface water. Although such algorithms may overlook spatial details in images, which can lead to inaccuracies in delineating water boundaries and identifying small water bodies or features, shallow classifiers such as Support Vector Machine (SVM) (S. Huang et al. 2018) and modified Statistical Region Merging (SRM) (Nock and Nielsen 2004) show improvements in accuracy and performance by incorporating some spatial information. In contrast, deep learning methods, applied to high resolution optical satellite imagery, aim to enhance the identification of intricate water bodies with diverse sizes and shapes (Cui et al. 2021; Duan and Hu 2020; Kang et al. 2021; Li et al. 2022; Yu et al. 2021; Yuan et al. 2021). Challenges, such as the meandering of water body boundaries, are addressed by techniques like Loss Function (Miao et al. 2018), designed to derive accurate water body boundaries by considering boundary weight distribution. Efficient post-processing algorithms further improve surface water detection (Chu et al. 2019; Sun et al. 2021).

Several surface water body detection datasets using satellite imagery exist, each serving specific purpose(s) and location(s). These include global datasets developed for flood emergency responses (Wieland et al. 2023), processing coastal satellite images into coastline morphology data (Seale et al. 2022), accurately segmenting water areas even in complex backgrounds and addressing challenges such as identifying small tributaries of rivers (Hu et al. 2022), and surface water detection (Li et al. 2023). Additionally, one dataset has been developed for environmental studies in particular locations, such as regions affected by climate change, e.g., the Arctic. The specifications of these datasets are summarized in Table 1. The major models and encoders used are U-Net (Ronneberger, Fischer, and Brox 2015), DeepLabV3+ (Chen et al. 2018), MobileNetV3 (Howard et al. 2019), ResNet-50 (He et al. 2016) EfficientNet-B4 (Tan and Le 2019), Fully Convolutional Networks (FCN) (Long, Shelhamer, and Darrell 2015), Multi-Branch

Aggregation (Weng et al. 2022), Feature Fusion Upsample (Y. Xu et al. 2021), CNN (Fukushima 1980), and Pyramid Consistency Loss (PCL) (Yue et al. 2019).

Many datasets for spotting surface waters (Hu et al. 2022; Isikdogan, Bovik, and Passalacqua 2020; Luo, Tong, and Hu 2021; Seale et al. 2022) use optical satellite images by Landsat-8 ("Landsat 8 | Landsat Science" 2021; "Landsat 8 | U.S. Geological Survey," n.d.) and Sentinel-2 ("Sentinel-2" 2023; "Sentinel-2 - Missions - Sentinel Online," n.d.)) with low spatial resolution, i.e., 15 and 10 m/pixel GSD, respectively, resulting in small rivers and lakes to appear blurry and hard to distinguish. Furthermore, some datasets (Li et al., 2023; Moortgat et al., 2022; Zhang et al., 2022) contain a limited number of images (see Table 1), potentially resulting in reduced applicability or restricted geographic scope, particularly even when they aim to cover large areas like the entire Earth, the Arctic, and the United States. A significant volume of images is essential to adequately represent the complexity and diversity of real-world conditions, thereby increasing the dataset's effectiveness for crucial research and policy-making purposes. Also, some studies are solely focused on specific applications like flood mapping (Wieland et al., 2023), or particular regions such as the Arctic (Moortgat et al., 2022) and coastal areas (Seale et al., 2022), which can cause limited scope and generalizability, insufficient geographic coverage, bias and overfitting, and underrepresentation of diverse water bodies. Using multi-channel imagery for water body detection often entails substantial computational resources and time compared with three standard (RGB) channel images. Finally, imprecise river edge detection in poor lighting and similar color conditions (Hu et al. 2022) and the inability to see through clouds (Isikdogan, Bovik, and Passalacqua 2020) are some added limitations reported in earlier studies.

There are just two datasets focused solely on the United States, and both come with shortcomings. Agriculture-Vision (Chiu et al. 2020) is a Land Use Land Cover (LULC) dataset having 94,986 512×512-pixel images with 0.1, 0.15, and 0.2 m/pixel GSD (i.e., the distance between two consecutive pixel centers measured on the ground), with a focus mainly on semantic segmentation of agricultural patterns across the United States. Although solely focused on the United States, the dataset has six distinct classes (including cloud shadow, double plant, planter skip, standing water, waterway, and weed cluster), two of which only specifically address surface water bodies. In addition, the dataset contains low-quality images, i.e., 130 pixels per inch (any image with fewer than 300 pixels per inch is considered a low-resolution image (pro-emi, 2023)) captured by UAV cameras like Canon SLR, Nikon D850, and Nikon D800E. Another dataset is UrbanWatch (Zhang et al. 2022), a LULC dataset with only 200 512×512 pixel and 1.0 m/pixel GSD images, focused on urban environments across 22 major cities in the United States, where surface water bodies are identified as one of the nine LULC classes (buildings, roads, parking lots, tree canopies, grass/shrub, water bodies, agriculture, barren land, and others) in the dataset. Here, the major source is the National Agriculture Imagery Program (NAIP) (Earth Resources Observation and Science (EROS) Center, 2017), which primarily uses aerial methods, such as aircraft equipped with film or digital cameras, to capture images. Neither dataset solely focuses on water bodies nor satellites used to collect images. Therefore, to our knowledge, no dedicated surface water body detection dataset exists for the United States.

Here, we present USS-Water, a dataset specifically developed for surface water body detection in the United States. This dataset, not intended for any specific application, includes 1,483 high-quality, three-channel (RGB) satellite images. These images were collected from 147 distinct locations across 44 states and are freely available from Google Earth. Each image has a resolution of 1,000×1,000 pixels and a high spatial resolution of 0.3 meters per pixel (GSD), the highest available GSD. The images cover diverse types of water bodies, including ocean coastlines, shipyards, rivers, ponds, lakes, creeks, and lagoons, to ensure broad applicability and generalizability across various geographic regions and types of water bodies.

Furthermore, in response to several key limitations observed in existing surface water body detection models, including excessive computational demands, the growing need for real-time applications, challenges in achieving accurate segmentation, inefficiencies in handling large datasets, and the complexity of using freely available data, we developed the U-Net+ model. We employed the water-body segmentation U-Net model originally developed by DEEPNETS as our foundation ("Water-Body Segmentation | UNet Model," n.d.). Building upon this base code, we conducted data preprocessing, introduced new layers to enhance the U-Net architecture, and generated graphical representations of the results. Our modifications have optimized the model for various segmentation tasks, significantly reducing computation time and enhancing memory efficiency, thereby making it suitable for real-time applications. This surface water body detection segmentation model, hereafter referred to as the U-Net+, harnesses the capabilities of Convolutional Neural Networks (CNNs) and U-Net architectures, prioritizing accuracy while mitigating computational complexity and processing duration. For instance, the U-Net+ accurately captures watercolor variations and surrounding terrain, precisely delineating boundaries for large water bodies like oceans and lakes. It can efficiently process large datasets while adapting to spectral and spatial disturbances, distinguishing water from non-water in shadowed areas using contextual information, thus enhancing its adaptability to different environmental conditions. Moreover, the model is designed to work seamlessly with freely available RGB satellite images, simplifying its use and making it accessible to a wide range of users.

The dataset (USS-Water) and the model (U-Net+) developed here hold significant value across various fields. The model proposed offers a user-friendly implementation, requiring users to simply upload an easily obtainable RGB image for analysis. By using freely available RGB satellite images from Google Earth, the combined dataset and model provide a cost-effective solution for surface water body detection. This solution makes surface water detection more accessible to a wide range of users and organizations. Researchers in environmental science, hydrology, remote sensing, and geospatial analysis can use the USS-Water dataset to study surface water bodies in the United States. Government agencies responsible for managing water, responding to disasters, and protecting the environment can improve their understanding of water dynamics, assess water quality, and predict and manage floods using both the dataset and the U-Net+ model. Policymakers can make informed decisions about water resources, land use, and infrastructure based on insights from the dataset and model. NGOs and conservation organizations focused on water conservation, habitat restoration, and biodiversity can identify

and prioritize areas for conservation efforts using the detailed water body delineations provided by the U-Net+ model. Emergency responders, including federal and local emergency management agencies, can use the dataset and model during floods and natural disasters for better situational awareness and response planning. Furthermore, agriculture, forestry, energy, and urban development companies can use the USS-Water dataset and the U-Net+ model for land use planning, site selection, and environmental assessments.

Table 1. Specifications of previously developed surface water detection datasets and models

Dataset	Model(s)	Publication Year	Water Body Types	Number of Images	Channels[a]	Image Size (pixel)	GSD[b] (m/pixel)	Number of Labeled Pixels (billion)	Image Source	Geographic Coverage	Acquisition	The Best-Performing Model Accuracy (F1%)[c]
Wieland et al. (Wieland et al. 2023)	U-Net and DeepLab-V3+ Encoder: MobileNet-V3, ResNet-50 and EfficientNet-B4	2023	Normal and flood water	1,120	4	2,048×2,048	0.8	4.69	IKONOS	Globe	Private	45.0 (U-Net with MobileNet-V3 encoder)
Moortgat et al. (Moortgat et al. 2022)	FCN Encoder: DeepWaterMap 2, L18 (ResNet, LinkNet) L34 (ResNet, LinkNet) U18 (U-Net, ResNet) and U34 (U-Net, ResNet)	2022	Rivers	142	4 (without additional bands) 8 (with additional bands)	10,000×10,000	1.2 0.5	14.20	GeoEye Quickbird-2/ WorldView-1/ WorldView-2 WorldView-3	Arctic	Private	84.9 (FCN with L18 encoder)
2020 GF challenge (Sun et al. 2021)	Faster-RCNN, YOLOv3, CRF, FPN and S^2 A-Net Encoder: ResNet-50+DCNv2, HRNet-W32, ResNet-50, ResNet101-V2 and DeepLab - V3+	2020	Rivers and lakes	1,000	3	492~2,000 ×492~2,000	0.8 4.0	0.24	GaoFen-2	-	Public	83.6 (RCNN+FPN with ResNet-50+DCNV2 and HRNet-W32 encoders)
SWED (Seale et al. 2022)	CNN Encoder: U-Net	2022	Coastlines of aquaculture	1,862	12	256×256	10.0	0.12	Sentinel-2	Globe	Public	92.0 (CNN with U-Net encoder)
ESKWB (Luo, Tong, and Hu 2021)	WatNet Encoder: MobileNet-V2 and DeepLab-V3+	2021	Lakes, rivers, reservoirs and seas	95	6	545~1,432 ×625~1,527	10.0	0.11	Sentinel-2	Globe	Public	93.7 (WatNet with MobileNet-V2 encoder)
WSD (Hu et al. 2022)	ResNet-50 with deep feature extraction, multi-branch aggregation and feature fusion upsample	2022	Rivers	16,320	3	256×256	30.0	1.07	Landsat-8 Google Earth	-	Private	96.8 (ResNet-50 with deep feature extraction, multi-branch aggregation and feature fusion upsample)
DeepWaterMap (Isikdogan, Bovik, and Passalacqua 2020)	DeepWaterMap-V2	2020	Rivers	140,000	6	-	30.0	-	Landsat-8	Globe	Public	93.0 (DeepWaterMap-V2)

UrbanWatch (Zhang et al. 2022)	FLUTE with Scale-aware Parsing Module (SPM), and View-aware Embedding Module (VEM)	2022	Water body	200	4	512×512	1.0	0.05	Aircraft	United States	Public	91.5 (FLUTE with Scale-aware Parsing Module (SPM) and View-aware Embedding Module (VEM)
GLH-Water (Li et al. 2023).	Pyramid Consistency Loss (PCL) Encoder: DeepLab-V3+, ResNet-50, FCN8s-VGG16 and PSPNet- ResNet-50	2023	Rivers, lakes and ponds in forests, irrigated fields, bare areas, and urban areas, glacial lakes	250	3	12,800x12,800	0.3	40.96	Google Earth	Globe	Public	90.2 (Pyramid Consistency Loss (PCL) with PSPNet-ResNet-50 encoder)
Agriculture-Vision (Chiu et al. 2020)	FPN Encoder: ResNet-50 and ResNet-101	2020	Water body and water way	94986	4	512×512	0.15 (2017) 0.10 (2018) 0.20 (2018) 0.10 (2019)	24.90	UAV camera	United States	Public	71.3 (FPN with ResNet-101 encoder)

[a] an image displayed on a computer screen, two-dimensional, has layers known as bands or channels, in addition to the rows and columns of pixels. These layers contribute to the overall composition and representation of the image.

[b] the distance between two consecutive pixel centers measured on the ground. The bigger the value of the image GSD, the lower the spatial resolution of the image and the less visible details.

[c] the F1 score is the harmonic mean of precision and recall. Thus, it symmetrically represents both precision and recall in one metric.

2. Methodology

2.1. Dataset Images Collection

To collect images from various locations across the United States, we preferred Google Earth over other commonly used satellite image sources like Sentinel-2 (*Sentinel-2 - Missions - Sentinel Online*, n.d.), GaoFen-2 ("Gaofen-2 Satellite Sensor | Satellite Imaging Corp," n.d.) or Landsat-8 ("Landsat 8 | U.S. Geological Survey," n.d.) due to its extensive global coverage, user-friendly interface, high-resolution imagery, cost-effectiveness, and historical imagery. To download images from Google Earth, we employed the segment-geospatial Python package (samgeo), developed by Wu and Osco (Q. Wu and Osco 2023). This package allowed us to input bounding box coordinates and zoom level into the tms_to_geotiff function (to convert Tile Map Service tiles into GeoTIFF format), enabling us to download high-resolution images of the desired location.

To ensure diversity of the dataset, we handpicked geographic coordinates during data collection, considering three main criteria:

(a) covering seven types of water bodies, including rivers, ponds, lakes, oceans, coastlines, creeks, and shipyards. We have chosen to limit our focus to these seven specific types of water bodies due to their distinct characteristics. From a satellite perspective, many other water body types appear similar. For instance, bays may be classified as part of ocean coastlines, and hot springs may closely resemble ponds. Therefore, we categorized all other water bodies into one of the primary water body classes for consistency and clarity in our analysis,

(b) representing a spectrum of geographic landscapes, including different land cover conditions, shapes of water bodies, and color tones,

(c) spanning a wide range of geographic locations to depict diverse environments across the country, including urban, suburban, and rural areas, as well as coastal regions, mountainous terrains, and plains.

The geographic coordinate selections are illustrated in Figure 1 and detailed in Table 2. We used 1,483 RGB images, each with 1,000×1,000 resolution and a GSD of 0.3 m/pixel (i.e., zoom level 19), to develop the surface water body detection dataset. We labeled every image in the dataset using a descriptive naming convention, offering users essential details regarding the image content. The naming convention comprises latitude and longitude coordinates, followed by the state, water body type, and a unique identifier. This format enables users to swiftly discern the location and type of water body depicted in the image, streamlining data management and interpretation processes.
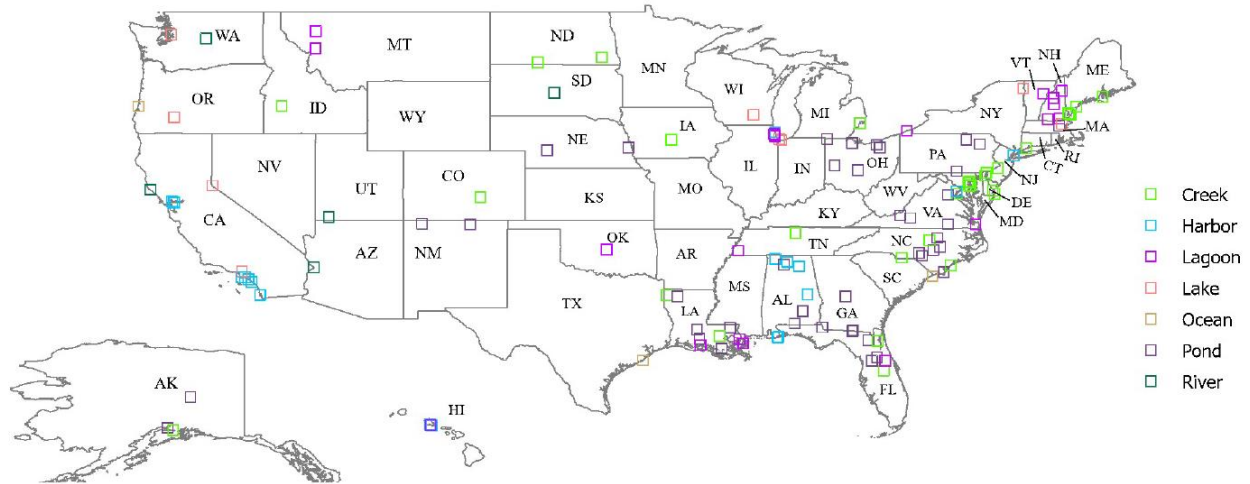
Figure 1: Geographical distribution of the images collected across the United States

Table 2: Number of satellite images collected by state and category

State	Creek[1]	Shipyard[2]	Lagoon[3]	Lake[4]	Ocean[5]	Pond[6]	River[7]	Total
Alabama		15				13		28
Alaska	2					14		16
Arizona							8	8
California		102		1			18	121
Colorado	4							4
Connecticut	6							6
Delaware	18							18
Florida	47		4			22		73
Georgia						19		19
Hawaii		45	3					48
Idaho	18							18
Illinois		14						14
Indiana				90				90
Iowa	4							4
Louisiana	2		16			11		29
Maine	36							36
Maryland	53							53
Massachusetts				2		30		32
Michigan	5							5
Mississippi			22					22
Montana			11					11
Nebraska						9		9
Nevada				8				8
New-Jersey	24							24

State								Total
New-Mexico		51				4		55
New-York		1		84				85
New Hampshire			44					44
North-Carolina	5					69		74
North-Dakota	8							8
Ohio						24		24
Oklahoma			4					4
Oregon				38	18			56
Pennsylvania			2			13		15
South-Carolina					109			109
South-Dakota							163	163
Tennessee	7		10					17
Texas					25			25
Utah							3	3
Vermont			14					14
Virginia	1	2	3			27		33
Washington				18			25	43
Wisconsin				15				15
Total	240	230	133	256	152	255	217	1483

[1] a small stream, often a tributary to a river (Taylor and Stokes 2005)
[2] a place where ships are built and repaired, typically adjacent to a body of water (Molland 2011)
[3] a shallow body of water separated from a larger sea or ocean by a barrier such as a sandbar or coral reef (Kjerfve 1986)
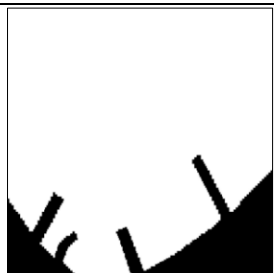[4] a large body of freshwater surrounded by land (Wetzel 2001)
[5] a vast and continuous body of salt water that covers more than 70% of the Earth's surface (Pinet 2019)
[6] a small body of still water, usually smaller than a lake (Wetzel 2001)
[7] a large, flowing body of water that usually empties into a sea or ocean (Taylor and Stokes 2005)
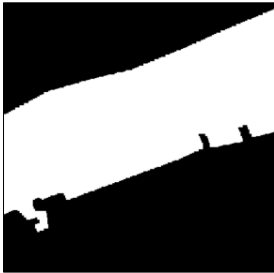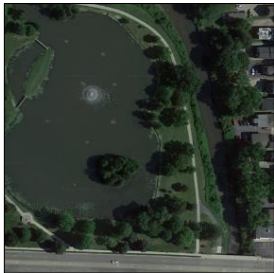
2.2. Annotation

The annotation process involved systematic labeling and verification. Initially, a researcher from our team manually delineated the boundaries of water bodies in each image using Label Studio ("Open Source Data Labeling," n.d.) to ensure accuracy during model training. Subsequently, another team member reviewed these annotations to verify precision, addressing any redundancies, omissions, or discrepancies identified during the process. Annotations that did not meet the required standards - ensuring that the annotated boundaries closely matched the actual edges of the water bodies, with complete coverage, correct classification, and no overlapping or gaps - were discarded, and the entire image was reannotated. The annotations were exported in COCO (Common Objects in Context) format, which is commonly used in computer vision tasks such as object detection, instance segmentation, and image classification. We then converted the COCO files into true binary mask images to facilitate more efficient handling and processing of segmentation data. Figure 2 illustrates the images and their corresponding masks depicting types of surface water bodies within the USS-Water dataset.

Original	Mask	Original	Mask
River		Ocean Coastline	
Pond		Lagoon	
Creek		Shipyard	
Lake			

Figure 2: Visualizing the images and their corresponding masks representing surface water bodies within the USS-Water dataset

2.3. Model Development

In this study, we used semantic segmentation in conjunction with the U-Net architecture to differentiate water body image pixels from other pixels in satellite imagery. Among a range of segmentation methodologies such as semantic segmentation (Guo et al. 2018), instance

segmentation (Hafiz and Bhat 2020), and panoptic segmentation (Kirillov et al. 2019), we specifically employed semantic segmentation, which assigns categorical labels to individual pixels within the image. The U-Net architecture demonstrates notable proficiency in semantic segmentation tasks, thus serving as our chosen framework for this analysis.

U-Net+ has been redesigned to enhance segmentation accuracy while reducing computational overhead and processing time, rendering it suitable for real-time applications. We achieved this by implementing compression techniques to decrease the number of pixels in the input image without compromising quality. Specifically, the function predict_masks is designed to handle large images by splitting them into 1000×1000-pixel patches, resizing these patches to 512×512 pixels for model prediction, and then processing the predicted mask back to the original patch size. This optimization reduced the total pixel count by 50%, halving the processing time and enhancing suitability for real-time water detection. Furthermore, only essential layers were retained in the architecture, streamlining the model and contributing to its computational efficiency. Additionally, U-Net+ requires only three-channel RGB images, which are readily available online, simplifying its use.

To ensure a fair distribution between training and test data, we randomly allocated 90% of the original image dataset to the training set, with the remaining 10% designated for the test set. Both the training and test sets included images from a variety of geographic regions, thereby guaranteeing the adequate representation of their spatial distribution. The effectiveness of this allocation strategy in maintaining regional diversity is evident in Figure 3, which depicts the geographic distribution of images in both the training and test sets, clearly showing the balanced representation and diversity of regions included in the dataset.
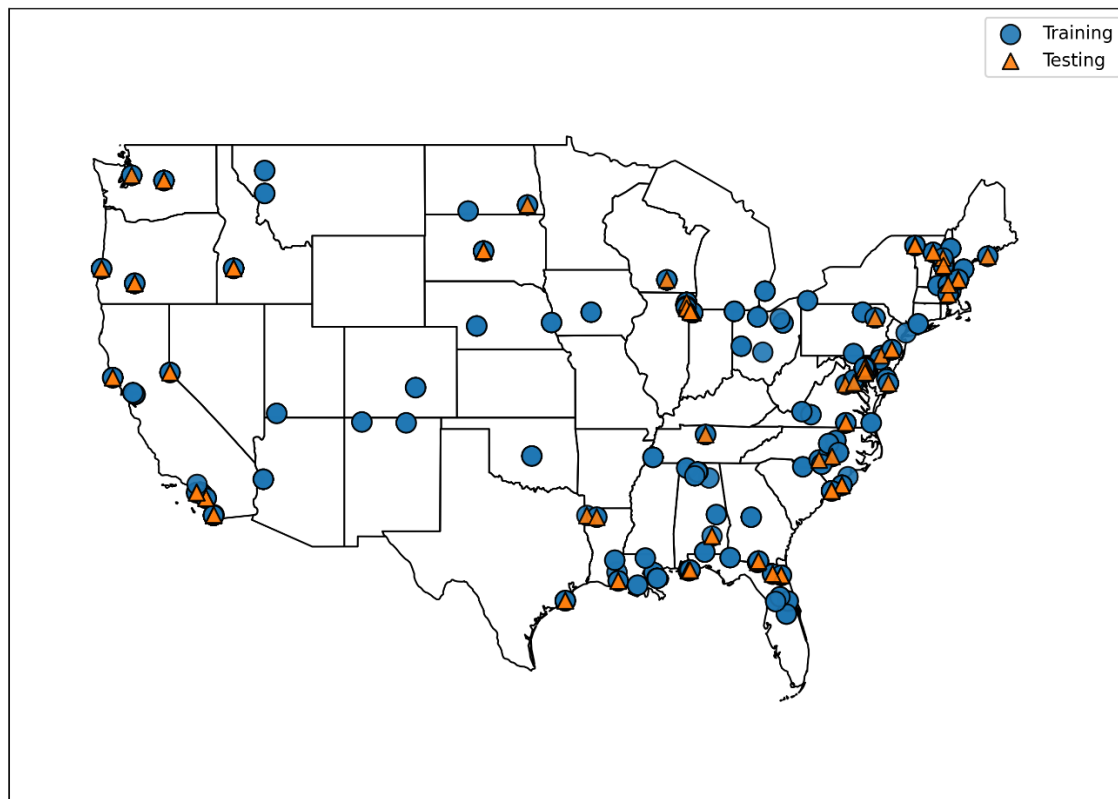
Figure 3: Geographic distribution of images used in the training and test sets

During the training process, we ensured the model's robustness against variations in input data by employing preprocessing and augmentation techniques. This allowed the model to tolerate spectral and spatial perturbations caused by different sensor characteristics and atmospheric conditions. For instance, the model can classify shadow pixels as water or non-water depending on the surrounding contextual information, enhancing its adaptability to diverse environmental settings. Once trained, the model predicts the water body. We improved the predicted mask by implementing post-processing on the first channel (index 0) of the multi-channel image (i.e., the predicted mask), where each represented either water or no water. We then performed thresholding on the selected channel, creating a binary mask where each pixel was true if its value exceeded 0.5 and false otherwise. We used a 0.5 threshold, common for predicted mask values ranging from 0 (non-water) to 1 (water) and converted the resulting binary mask's Boolean values to integers (true to 1, false to 0) for easier processing or visualization.

Finally, from a user perspective, the U-Net+ model offers ease of use; users provide the image, and the model automatically adjusts dimensions and size, ensuring seamless processing. A schematic representation of the U-Net-based convolutional neural network architecture, i.e., U-Net+, used to segment pixels into water and non-water classes is provided in Figure 4.
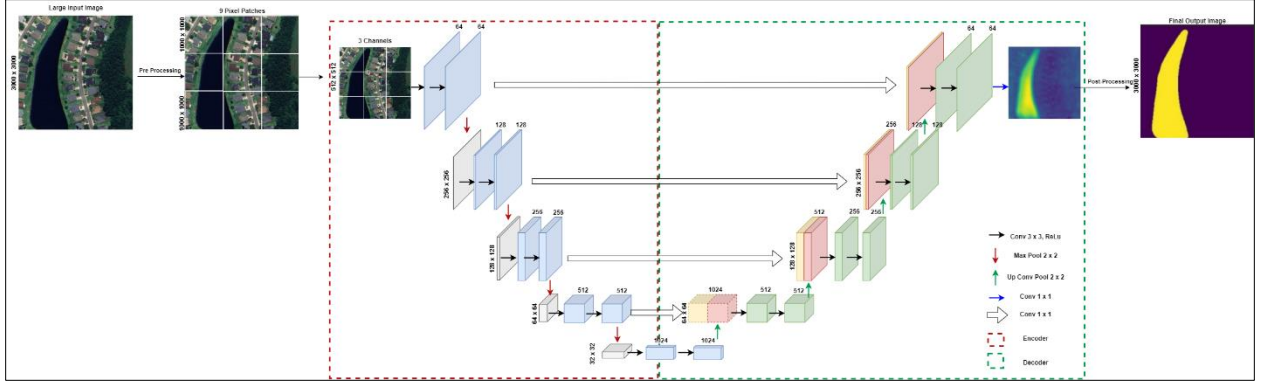
Figure 4: A schematic representation of the U-Net-based convolutional neural network architecture used to segment pixels into water and non-water classes

2.4. Model Training and Validation

In addition to U-Net+, we trained two existing segmentation models, DeepLabV3+ (Chen et al. 2018) and MSResNet (Liu et al. 2019), as the baseline models using our dataset. Compared to other commonly used segmentation models such as Fully Convolutional Networks (FCNs) (Long, Shelhamer, and Darrell 2015), PSPNet (Zhao et al. 2017) EfficientNet (Tan and Le 2019), these models offer distinct advantages. DeepLabV3+ efficiently captures the diverse dimensions and configurations of water bodies, uses unlabeled data, and incorporates self-supervised learning to enhance stability and performance. Similarly, MSResNet excels in capturing multi-scale features through residual connections and multi-scale context aggregation, ensuring robust segmentation performance, and preserving image details for higher accuracy. We validated U-Net+, DeepLabV3+, and MSResNet with a test set of 10% randomly selected samples from the USS-Water dataset. The evaluation involved comparative quantitative analysis using performance metrics, including Intersection over Union (IOU), precision, recall, and F1-score. We performed qualitative analysis as well, which involves analyzing non-numeric data, i.e., here images, to gain deeper insights into the U-Net+ as well as the baseline models capabilities beyond numerical metrics (marie 2023; "A Detailed Exploration of Qualitative Research (with Examples)," n.d.; "What Is Qualitative Data? Types, Examples & Analysis | Fullstory," n.d.).
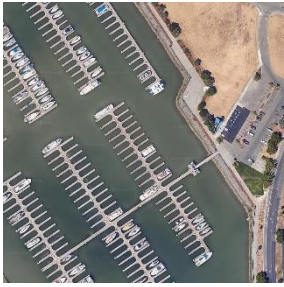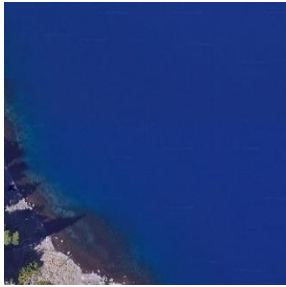
3. Results

3.1. Dataset

The USS-Water Dataset contains 1,483 images with 1000×1000 pixels and 0.3 meters GSD. These compact image dimensions allow for the capture of intricate details while ensuring a manageable size (this smaller dimension accelerates processing times with existing methodologies), and abundant sampling with over 1.48 billion labeled pixels establishes the present dataset as the largest available for surface water detection in the United States. Our dataset includes images from 147 unique locations across 44 states, covering seven major water bodies: ocean coastlines, shipyards, rivers, ponds, lakes, creeks, and lagoons. Each image retains

essential data points such as location coordinates, state names, and water body types, as presented in Figure 5.

	43.5617272541, -124.2125971787_Oregon_Ocean_270		28.9570126095, -95.2603580446_Texas_Ocean_578
	33.61343072777256, -117.90283689626185_California_Harbor_960		38.10713592630591, -122.26815811975217_California_Harbor_1354
	37.195776, -113.282703_Utah_River_889		47.45100696, -120.3196986089_Washington_River_473
	39.891160747665324, -82.91125749775279_Ohio_Pond_409		38.46166690429156, -77.75035153952265_Virginia_Pond_542
	42.9208987628, -122.1500879551_Oregon_Lake_327		44.5874065212, -73.4199598281_New-York_Lake_1313

	41.64056206503612, -93.64147558746981_ Iowa_Creek_584		43.53334830609714 , - 70.36664904928217 _Maine_Creek_1009
	42.86534406079449, - 71.3347353285942_ NewHampshire_Lag oon_133		44.03708154099185 6, - 71.67435806198735 _NewHampshire_La goon_841

Figure 5: USS-Water dataset sample images. Image label contains longitude, latitude, state, class, and unique identifier.

3.2. Model Accuracy

Table 3 presents the benchmark results of the baseline and the U-Net+ models on USS-Water test set. It is observed that MSResNet achieved an IOU score of 84.1%, surpassing U-Net+ and DeepLabv3+, which reached scores of 83.2% and 81.6%, respectively. However, despite MSResNet exhibiting the highest quantitative score, it demonstrated relatively lower performance in qualitative assessment. Figures 6 and 7 illustrate this observation, showing that U-Net+ consistently outperforms both MSResNet and DeepLabV3+ in distinguishing intricate features of water bodies, excels in detecting narrow and elongated water bodies, and maintains higher consistency across diverse types of water bodies. While DeepLabV3+ and MSResNet occasionally exhibit robust performance in certain scenarios, such as high-contrast or well-defined water bodies, their performance tends to degrade in more challenging conditions. U-Net+'s robust architecture and effective post-processing steps enable it to handle these variations better, resulting in more reliable and accurate segmentation across the board.

Table 3: Benchmark results of baseline models and the proposed model on USS-Water test set

Model	Backbone	IOU	Precision	Recall	F1-Score
U-Net+	U-Net	83.2%	0.98	0.88	93.6 %
DeepLabV3+	DeepLabv3+	81.6 %	0.90	0.95	92.0 %

MSResNet	ResNet-34	84.1 %	0.96	0.94	95.4 %

3.3. Model Outcomes

This section analyzes the outcomes of applying the U-Net+ model to the USS-Water dataset, with a comparative evaluation against DeepLabV3+ and MSResNet models. The segmentation results in Figure 6 highlight the effectiveness of the U-Net+ model in accurately identifying diverse types of water bodies. For large and distinct water bodies such as ocean coastlines and lakes, U-Net+ exhibits high precision in delineating boundaries. For instance, in the case of ocean coastlines, U-Net+ effectively distinguishes between water and land, a crucial capability for coastal management and environmental monitoring applications. Similarly, when segmenting lakes, U-Net+ captures variations in watercolor and surrounding terrain with high accuracy. These results affirm the model's robustness in handling large and complex water bodies, aligning with findings from related studies that emphasize the importance of advanced segmentation techniques in such contexts.

When tested with challenges in more intricate scenarios, such as narrow rivers and creeks where boundaries are less distinct, U-Net+ demonstrated commendable accuracy, closely matching the ground truth (i.e., the accurate and verified information about the actual boundaries of the water bodies, as observed in the real world) and minimizing discrepancies. This performance is critical for applications like river monitoring and flood prediction, where precise boundary detection is essential. The inclusion of post-processing techniques further enhanced the segmentation quality by reducing noise and refining water boundaries, thus ensuring high-quality outputs across various water body types.

Figure 7 offers a comparative analysis of the predictions generated by U-Net+, DeepLabV3+, and MSResNet models. This comparison highlights that while all three models perform well in simpler scenarios, U-Net+ maintained robust performance across diverse conditions. DeepLabV3+ occasionally outperformed U-Net+ in challenging environments with mixed features or low contrast, highlighting its advanced architecture's benefits. For example, DeepLabV3+ produced highly accurate results with minimal errors in the segmentation of shipyards and lagoons, demonstrating its robustness in complex settings.
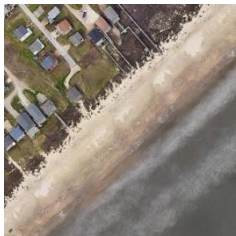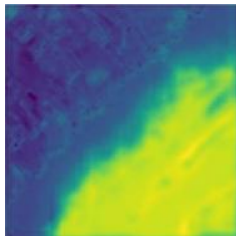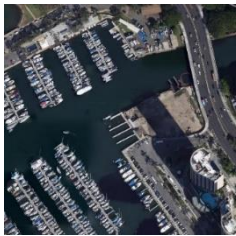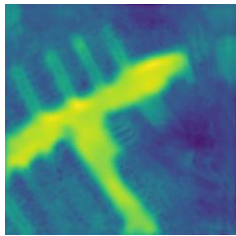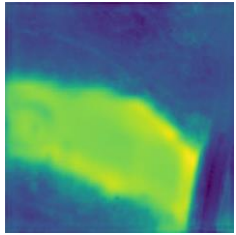
U-Net+ exhibited significant strengths in most scenarios, showing its versatility and effectiveness. Although it struggled with false positives in complex backgrounds or noisy images, post-processing steps mitigated these issues. Compared to MSResNet, which often under-segmented or over-segmented water bodies, U-Net+ consistently delivered reliable performance, reinforcing its suitability for various water body detection applications.
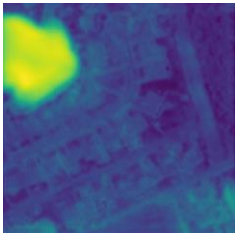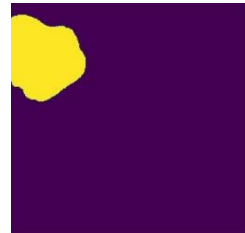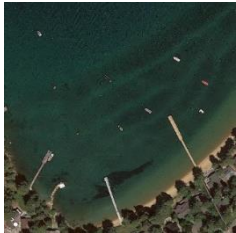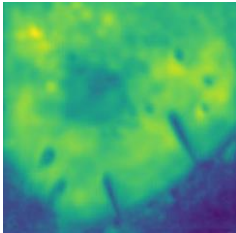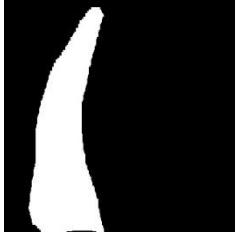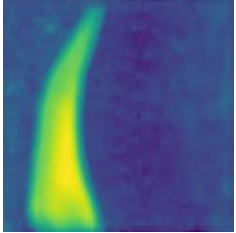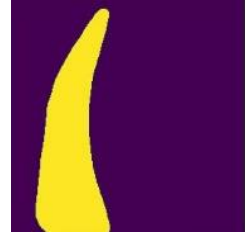
In comparison to other models, U-Net+ has several advantages. First, U-Net+ uses a comprehensive and diverse dataset, ensuring the model is trained on a wide range of scenarios, which enhances its generalizability. Second, detailed evaluation metrics, including Intersection over Union (IoU), precision, and recall, thoroughly assess U-Net+'s performance, offering a clear

benchmark for future research. Third, the focus on real-world challenges, such as detecting water bodies in noisy and low-contrast environments, highlights the practical applicability of U-Net+.

To further improve U-Net+, future work should consider incorporating multi-scale feature extraction techniques and additional spectral bands like NIR, which have been shown to enhance segmentation accuracy in other studies. Advanced post-processing methods and robust noise-handling techniques could also improve the model's performance in challenging environments. Expanding the validation set to include more varied geographic regions would provide a more comprehensive assessment of U-Net+'s robustness and reliability.

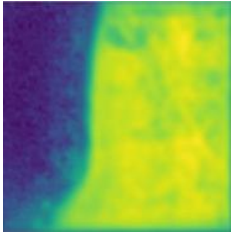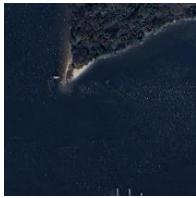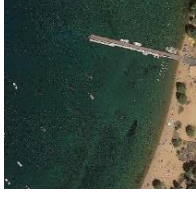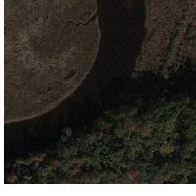In conclusion, the model outcomes illustrated in Figures 6 and 7 demonstrate the efficacy of U-Net+ in water body segmentation. The model exhibits significant strengths across various scenarios, enhancing its performance by effective post-processing. The comparative analysis with DeepLabV3+ and MSResNet underscores U-Net+'s robustness and versatility. Incorporating insights from recent studies, such as multi-scale feature extraction and advanced post-processing, can further enhance U-Net+'s performance and reliability, making it a valuable tool for a wide range of applications in water body detection and environmental monitoring.

Class	Original Image	Ground Truth	U-Net+ Model Prediction	Post-processing
Ocean Coastlines				
Shipyard				
Rivers				

Figure 6: Samples of seven classes of images in original, ground truth, U-Net+ predicted and post-processed format

Class	Original	Ground Truth	Post-processed		
			U-Net+	**DeepLabv3+**	**MSResNet**
Shipyard					

Figure 7: Qualitative comparison of U-Net+, DeepLabv3+ and MSResNet models

3.4. Limitations

Although our model performs well, it has several limitations. First, since it was trained exclusively on the USS-Water dataset, it struggled to predict water bodies in other parts of the world. Second, the model was trained solely on satellite images, which are top-down views. As a result, it performed poorly when given eye-level images of water bodies. Lastly, we randomly split our dataset into training and test sets during training. This random split could have

introduced bias, affecting the model's accuracy and generalization. These limitations highlight areas for improvement to enhance the model's performance and versatility.

4. Case Study

In our case study, we undertook the challenge of analyzing a complex area that we could not directly feed into the model as it exceeded typical GPU memory constraints due to its large scale. To tackle this issue, we adopted a strategic approach that divided the area into smaller patches, as discussed in section 2.3, reducing the pixel count by 50% and halving the processing time for such large images.

For our case study, we selected two unique and complex areas. The first area was downtown Chicago. As the third largest city in the United States, Chicago's unique architecture and diverse water bodies present a perfect challenge for U-Net+ to predict accurately, as presented in Figure 8(a). The second area was the Gary Community School Corporation area in Gary, Indiana. This location was particularly challenging due to its thin canal and scattered dry areas, which tested the model's ability to precisely identify water bodies and eliminate dry regions. Additionally, the Gary area's various shades and dark land tested the model's robustness, as illustrated in Figure 9(a). Table 4 presents the locations, coordinates, image sizes, and dimensions of the pilot study areas' satellite images. Figures 8(b) and 9(b) show the U-Net+ model's high accuracy despite the complexities of the study area. The U-Net+ model showed impressive accuracy in predicting lakes, ponds, and shipyard areas, even in a challenging study area. The model successfully distinguished boats in the water (see Figure 8(b)) and accurately identified thin rivers and complex water bodies (see Figure 9(b)).

Our case study tested the robustness of our U-Net+ model. It guided the construction and further development of the model by highlighting its ability to accurately predict and delineate complex water bodies in large-scale images, even in challenging environments. Given the complexity of surface water detection tasks, the case study serves as an example for others to build upon this model, demonstrating how it can be adapted and enhanced for various applications.

Table 4: Locations, coordinates, image sizes, and dimensions of the pilot study areas satellite images

Location Name	Jackson Park, Chicago, IL	Gary Community School Corporation, Gary, IN
Location Coordinates	41.78366585885544, -87.57999001264847	41.612898753320216, -87.30889155863774
Image Size on Disk (MB)	86.2	325
Dimensions (pixel)	8,368×7,977	21,904×12,236

| (a) | (b) |
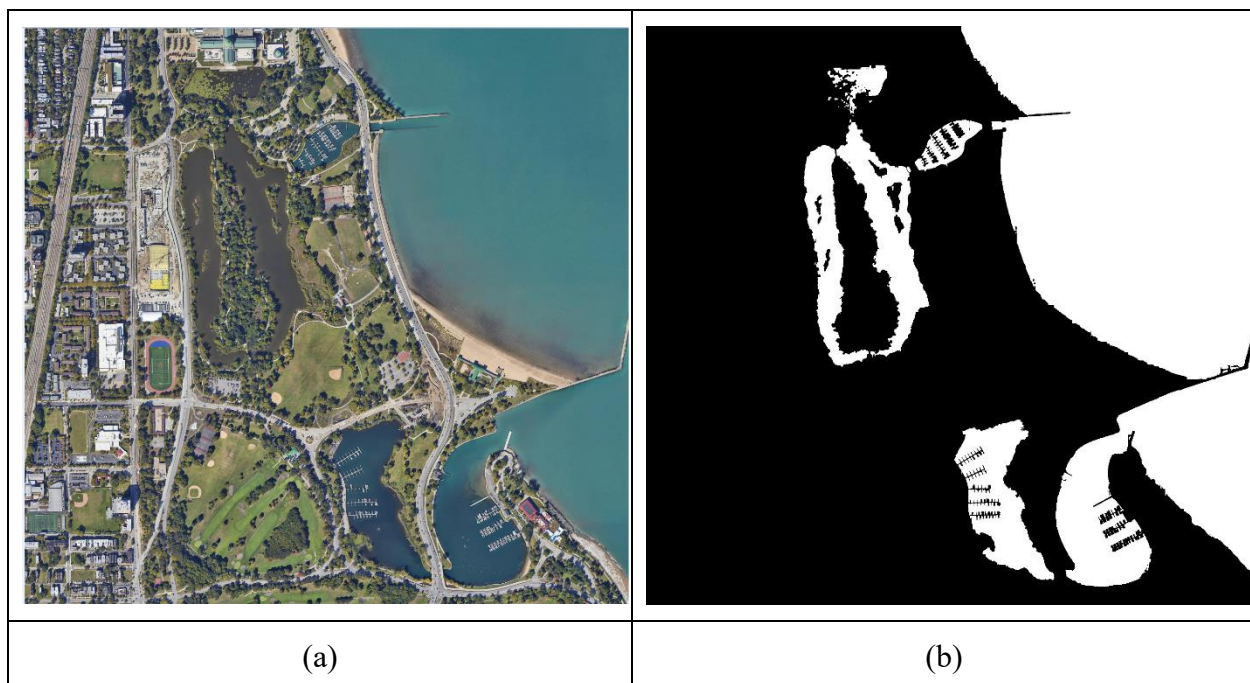
Figure 8: Jackson Park, Chicago, IL, USA, (a) original image, (b) predicate mask by the U-Net+ model
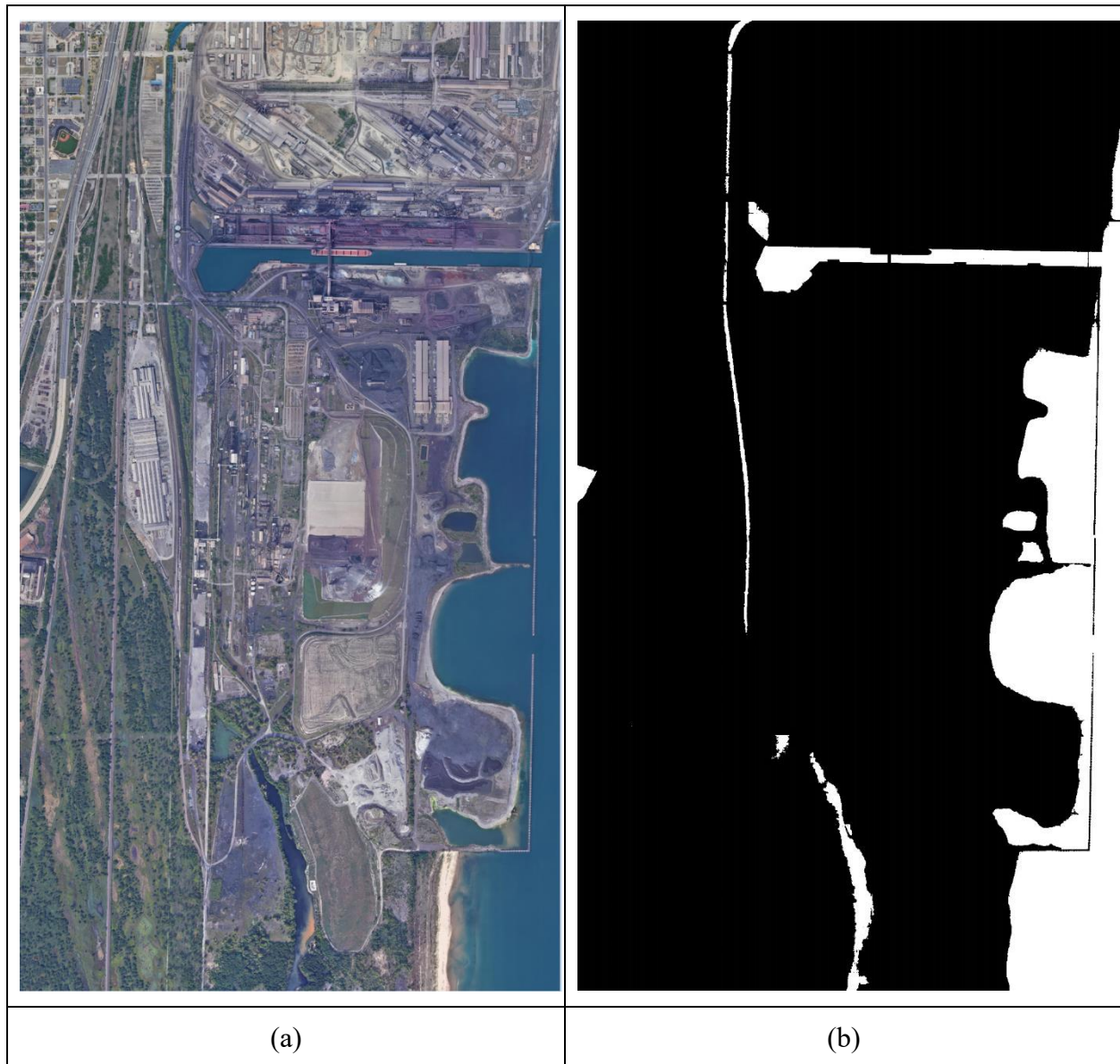
Figure 9: Gary Community School Corporation, Gary, IN, USA, (a) original image, (b): predicate mask by the U-Net+ model

5. Conclusion

The development of the USS-Water dataset and the U-Net+ model marks a significant advancement in surface water detection using high-resolution satellite imagery. The USS-Water dataset, with its 1483 high-quality RGB images covering a wide array of water bodies across 44 states, provides an extensive and diverse resource for researchers and practitioners. Each image's high spatial resolution of 0.3 meters per pixel ensures detailed and precise representation, making the dataset particularly valuable for various applications in environmental monitoring, water resource management, and disaster response.

The U-Net+ model, an enhancement of the traditional U-Net architecture, has been meticulously designed to address the complexities of water body segmentation. By introducing new layers and optimizing the U-Net architecture, the U-Net+ model achieves higher segmentation accuracy while reducing computational overhead. This is particularly beneficial for real-time applications, where processing speed and accuracy are critical. The model's ability to accurately delineate water bodies, even in challenging scenarios like varying watercolor, surrounding terrain, and shadowed areas, demonstrates its robustness and versatility.

Comparative evaluations against DeepLabV3+ and MSResNet models highlight the superior performance of U-Net+. With an Intersection over Union (IoU) score of 83.2%, precision of 0.98, recall of 0.88, and an F1-score of 93.6%, U-Net+ not only meets but often exceeds the performance of its counterparts. The detailed analysis reveals that while MSResNet achieves a slightly higher IoU score of 84.1%, U-Net+ consistently delivers better qualitative results, particularly in complex and varied environments. The robust architecture and effective post-processing steps of U-Net+ enable it to handle diverse conditions, making it a reliable tool for accurate water body segmentation.

The practical implications of this work are vast. For environmental scientists and hydrologists, the USS-Water dataset and U-Net+ model provide an essential tool for studying and monitoring surface water bodies. Government agencies can leverage these resources for better water resource management, disaster response planning, and environmental protection initiatives. Policymakers can make informed decisions based on accurate and detailed water body data, ensuring sustainable land and water use practices. NGOs and conservation organizations can identify and prioritize areas for conservation efforts, using the detailed delineations provided by U-Net+. Furthermore, companies in agriculture, forestry, energy, and urban development can use these tools for land use planning, site selection, and environmental assessments.

The case studies of downtown Chicago and the Gary Community School Corporation area in Gary, Indiana, demonstrate the practical application and effectiveness of the U-Net+ model in real-world scenarios. The model's ability to accurately predict and delineate complex water bodies in large-scale images underscores its applicability and reliability in diverse settings.

In conclusion, the USS-Water dataset and U-Net+ model represent a significant contribution to the fields of remote sensing and water body detection. The accessibility of the dataset and the model encourages further research and development, fostering advancements in environmental monitoring and resource management. Future work can build upon this foundation by incorporating additional spectral bands, enhancing post-processing techniques, and expanding the dataset to include more geographic regions, further improving the accuracy and applicability of surface water detection models.

Availability of Data and Materials

The U-Net+ model and the USS-Water database are available at

https://drive.google.com/drive/folders/1JDQmc6sCvQQz4bWA6aBOOw9YeglcaAgE?usp=sharing

https://github.com/NischalRam/USS--Water-Remote-Sensing-for-Water-Detection.git

References:

"A Detailed Exploration of Qualitative Research (with Examples)." n.d. Qualtrics. Accessed July 14, 2024. https://www.qualtrics.com/experience-management/research/qualitative-research/.

Becker-Reshef, Inbal, Chris Justice, Mark Sullivan, Eric Vermote, Compton Tucker, Assaf Anyamba, Jen Small, et al. 2010. "Monitoring Global Croplands with Coarse Resolution Earth Observations: The Global Agriculture Monitoring (GLAM) Project." *Remote Sensing* 2 (6): 1589–1609. https://doi.org/10.3390/rs2061589.

Behnamian, Amir, Sarah Banks, Lori White, Brian Brisco, Koreen Millard, Jon Pasher, Zhaohua Chen, Jason Duffe, Laura Bourgeau-Chavez, and Michael Battaglia. 2017. "Semi-Automated Surface Water Detection with Synthetic Aperture Radar Data: A Wetland Case Study." *Remote Sensing* 9 (12): 1209. https://doi.org/10.3390/rs9121209.

Chen, Liang-Chieh, Yukun Zhu, George Papandreou, Florian Schroff, and Hartwig Adam. 2018. "Encoder-Decoder with Atrous Separable Convolution for Semantic Image Segmentation." In *Computer Vision – ECCV 2018*, edited by Vittorio Ferrari, Martial Hebert, Cristian Sminchisescu, and Yair Weiss, 11211:833–51. Lecture Notes in Computer Science. Cham: Springer International Publishing. https://doi.org/10.1007/978-3-030-01234-2_49.

Chiu, Mang Tik, Xingqian Xu, Yunchao Wei, Zilong Huang, Alexander Schwing, Robert Brunner, Hrant Khachatrian, et al. 2020. "Agriculture-Vision: A Large Aerial Image Database for Agricultural Pattern Analysis." arXiv. https://doi.org/10.48550/arXiv.2001.01306.

Chu, Zhengquan, Tian Tian, Ruyi Feng, and Lizhe Wang. 2019. "Sea-Land Segmentation with Res-UNet And Fully Connected CRF." In , 3840–43. https://doi.org/10.1109/IGARSS.2019.8900625.

Cooley, Sarah W., Laurence C. Smith, Leon Stepan, and Joseph Mascaro. 2017. "Tracking Dynamic Northern Surface Water Changes with High-Frequency Planet CubeSat Imagery." *Remote Sensing* 9 (12): 1306. https://doi.org/10.3390/rs9121306.

Coskun, H. Gonca, Ozlem Gulergun, and Levent Yilmaz. 2006. "Monitoring of Protected Bands of Terkos Drinking Water Reservoir of Metropolitan Istanbul near the Black Sea Coast Using Satellite Data." *International Journal of Applied Earth Observation and Geoinformation* 8 (1): 49–60. https://doi.org/10.1016/j.jag.2005.06.003.

Cui, Binge, Wei Jing, Ling Huang, Zhongrui Li, and Yan Lu. 2021. "SANet: A Sea–Land Segmentation Network Via Adaptive Multiscale Feature Learning." *IEEE Journal of Selected Topics in Applied Earth Observations and Remote Sensing* 14:116–26. https://doi.org/10.1109/JSTARS.2020.3040176.

Donchyts, Gennadii, Fedor Baart, Hessel Winsemius, Noel Gorelick, Jaap Kwadijk, and Nick van de Giesen. 2016. "Earth's Surface Water Change over the Past 30 Years." *Nature Climate Change* 6 (9): 810–13. https://doi.org/10.1038/nclimate3111.

Duan, Lunhao, and Xiangyun Hu. 2020. "Multiscale Refinement Network for Water-Body Segmentation in High-Resolution Satellite Imagery." *IEEE Geoscience and Remote Sensing Letters* 17 (4): 686–90. https://doi.org/10.1109/LGRS.2019.2926412.

Earth Resources Observation And Science (EROS) Center. 2017. "National Agriculture Imagery Program (NAIP)." Tiff. U.S. Geological Survey. https://doi.org/10.5066/F7QN651G.

Fukushima, Kunihiko. 1980. "Neocognitron: A Self-Organizing Neural Network Model for a Mechanism of Pattern Recognition Unaffected by Shift in Position." *Biological Cybernetics* 36 (4): 193–202. https://doi.org/10.1007/BF00344251.

"Gaofen-2 Satellite Sensor | Satellite Imaging Corp." n.d. Accessed February 28, 2024. https://www.satimagingcorp.com/satellite-sensors/gaofen-2/.

Goward, Samuel N., Jeffrey G. Masek, Darrel L. Williams, James R. Irons, and R. J. Thompson. 2001. "The Landsat 7 Mission: Terrestrial Research and Applications for the 21st Century." *Remote Sensing of Environment*, Landsat 7, 78 (1): 3–12. https://doi.org/10.1016/S0034-4257(01)00262-0.

Guo, Yanming, Yu Liu, Theodoros Georgiou, and Michael S. Lew. 2018. "A Review of Semantic Segmentation Using Deep Neural Networks." *International Journal of Multimedia Information Retrieval* 7 (2): 87–93. https://doi.org/10.1007/s13735-017-0141-z.

Hafiz, Abdul Mueed, and Ghulam Mohiuddin Bhat. 2020. "A Survey on Instance Segmentation: State of the Art." *International Journal of Multimedia Information Retrieval* 9 (3): 171–89. https://doi.org/10.1007/s13735-020-00195-x.

He, Kaiming, Xiangyu Zhang, Shaoqing Ren, and Jian Sun. 2016. "Deep Residual Learning for Image Recognition." In , 770–78. https://openaccess.thecvf.com/content_cvpr_2016/html/He_Deep_Residual_Learning_CVPR_2016_paper.html.

Howard, Andrew, Mark Sandler, Grace Chu, Liang-Chieh Chen, Bo Chen, Mingxing Tan, Weijun Wang, et al. 2019. "Searching for MobileNetV3." In , 1314–24. https://openaccess.thecvf.com/content_ICCV_2019/html/Howard_Searching_for_MobileNetV3_ICCV_2019_paper.html.

Hu, Kai, Meng Li, Min Xia, and Haifeng Lin. 2022. "Multi-Scale Feature Aggregation Network for Water Area Segmentation." *Remote Sensing* 14 (1): 206. https://doi.org/10.3390/rs14010206.

Huang, Chang, Yun Chen, Shiqiang Zhang, and Jianping Wu. 2018. "Detecting, Extracting, and Monitoring Surface Water From Space Using Optical Sensors: A Review." *Reviews of Geophysics* 56 (2): 333–60. https://doi.org/10.1029/2018RG000598.

Huang, Shujun, Nianguang Cai, Pedro Penzuti Pacheco, Shavira Narrandes, Yang Wang, and Wayne Xu. 2018. "Applications of Support Vector Machine (SVM) Learning in Cancer Genomics." *Cancer Genomics & Proteomics* 15 (1): 41–51.

Isikdogan, Leo F., Alan Bovik, and Paola Passalacqua. 2020. "Seeing Through the Clouds With DeepWaterMap." *IEEE Geoscience and Remote Sensing Letters* 17 (10): 1662–66. https://doi.org/10.1109/LGRS.2019.2953261.

Justice, C.O, J.R.G Townshend, E.F Vermote, E Masuoka, R.E Wolfe, N Saleous, D.P Roy, and J.T Morisette. 2002. "An Overview of MODIS Land Data Processing and Product Status." *Remote Sensing of Environment* 83 (1–2): 3–15. https://doi.org/10.1016/S0034-4257(02)00084-6.

Kang, Jian, Haiyan Guan, Daifeng Peng, and Ziyi Chen. 2021. "Multi-Scale Context Extractor Network for Water-Body Extraction from High-Resolution Optical Remotely Sensed Images." *International Journal of Applied Earth Observation and Geoinformation* 103 (December):102499. https://doi.org/10.1016/j.jag.2021.102499.

Kirillov, Alexander, Kaiming He, Ross Girshick, Carsten Rother, and Piotr Dollar. 2019. "Panoptic Segmentation." In , 9404–13. https://openaccess.thecvf.com/content_CVPR_2019/html/Kirillov_Panoptic_Segmentation_CVPR_2019_paper.html.

Kjerfve, Björn. 1986. "COMPARATIVE OCEANOGRAPHY OF COASTAL LAGOONS." In *Estuarine Variability*, edited by Douglas A. Wolfe, 63–81. Academic Press. https://doi.org/10.1016/B978-0-12-761890-6.50009-5.

"Landsat 8 | Landsat Science." 2021. November 30, 2021. https://landsat.gsfc.nasa.gov/satellites/landsat-8/.

"Landsat 8 | U.S. Geological Survey." n.d. Accessed January 29, 2024. https://www.usgs.gov/landsat-missions/landsat-8.

Li, Yansheng, Bo Dang, Wanchun Li, and Yongjun Zhang. 2023. "GLH-Water: A Large-Scale Dataset for Global Surface Water Detection in Large-Size Very-High-Resolution Satellite Imagery." arXiv. http://arxiv.org/abs/2303.09310.

Li, Yansheng, Bo Dang, Yongjun Zhang, and Zhenhong Du. 2022. "Water Body Classification from High-Resolution Optical Remote Sensing Imagery: Achievements and Perspectives." *ISPRS Journal of Photogrammetry and Remote Sensing* 187 (May):306–27. https://doi.org/10.1016/j.isprsjprs.2022.03.013.

Liu, Bing, Qiao Liu, Taiping Zhang, and Yong Yang. 2019. "MSSTResNet-TLD: A Robust Tracking Method Based on Tracking-Learning-Detection Framework by Using Multi-

Scale Spatio-Temporal Residual Network Feature Model." *Neurocomputing* 362 (October):175–94. https://doi.org/10.1016/j.neucom.2019.07.024.

Long, Jonathan, Evan Shelhamer, and Trevor Darrell. 2015. "Fully Convolutional Networks for Semantic Segmentation." In , 3431–40. https://openaccess.thecvf.com/content_cvpr_2015/html/Long_Fully_Convolutional_Networks_2015_CVPR_paper.html.

Luo, Xin, Xiaohua Tong, and Zhongwen Hu. 2021. "An Applicable and Automatic Method for Earth Surface Water Mapping Based on Multispectral Images." *International Journal of Applied Earth Observation and Geoinformation* 103 (December):102472. https://doi.org/10.1016/j.jag.2021.102472.

marie. 2023. "What Is Qualitative Data? Exploring Its Meaning and Applications." Contentsquare. August 22, 2023. https://contentsquare.com/blog/qualitative-data/.

Markham, Brian L., and Dennis L. Helder. 2012. "Forty-Year Calibrated Record of Earth-Reflected Radiance from Landsat: A Review." *Remote Sensing of Environment* 122 (July):30–40. https://doi.org/10.1016/j.rse.2011.06.026.

Mateo-Garcia, Gonzalo, Joshua Veitch-Michaelis, Lewis Smith, Silviu Vlad Oprea, Guy Schumann, Yarin Gal, Atılım Güneş Baydin, and Dietmar Backes. 2021. "Towards Global Flood Mapping Onboard Low Cost Satellites with Machine Learning." *Scientific Reports* 11 (1): 7249. https://doi.org/10.1038/s41598-021-86650-z.

McFEETERS, S. K. 1996. "The Use of the Normalized Difference Water Index (NDWI) in the Delineation of Open Water Features." *International Journal of Remote Sensing* 17 (7): 1425–32. https://doi.org/10.1080/01431169608948714.

Miao, Ziming, Kun Fu, Hao Sun, Xian Sun, and Menglong Yan. 2018. "Automatic Water-Body Segmentation From High-Resolution Satellite Images via Deep Networks." *IEEE Geoscience and Remote Sensing Letters* 15 (4): 602–6. https://doi.org/10.1109/LGRS.2018.2794545.

Molland, Anthony F. 2011. *The Maritime Engineering Reference Book: A Guide to Ship Design, Construction and Operation*. Elsevier.

Nock, R., and F. Nielsen. 2004. "Statistical Region Merging." *IEEE Transactions on Pattern Analysis and Machine Intelligence* 26 (11): 1452–58. https://doi.org/10.1109/TPAMI.2004.110.

"Open Source Data Labeling." n.d. Label Studio. Accessed February 28, 2024. https://labelstud.io/.

Pekel, Jean-François, Andrew Cottam, Noel Gorelick, and Alan S. Belward. 2016. "High-Resolution Mapping of Global Surface Water and Its Long-Term Changes." *Nature* 540 (7633): 418–22. https://doi.org/10.1038/nature20584.

Perumal, Thinagaran, Md Nasir Sulaiman, and C. Y. Leong. 2015. "Internet of Things (IoT) Enabled Water Monitoring System." In *2015 IEEE 4th Global Conference on Consumer Electronics (GCCE)*, 86–87. https://doi.org/10.1109/GCCE.2015.7398710.

Pinet, Paul R. 2019. *Invitation to Oceanography*. Jones & Bartlett Learning.

pro-emi. 2023. "Difference between High Resolution vs Low Resolution Images." *PGBS* (blog). April 21, 2023. https://www.proglobalbusinesssolutions.com/low-resolution-and-high-resolution-images-difference/.

Ronneberger, Olaf, Philipp Fischer, and Thomas Brox. 2015. "U-Net: Convolutional Networks for Biomedical Image Segmentation." In *Medical Image Computing and Computer-Assisted Intervention – MICCAI 2015*, edited by Nassir Navab, Joachim Hornegger, William M. Wells, and Alejandro F. Frangi, 234–41. Cham: Springer International Publishing. https://doi.org/10.1007/978-3-319-24574-4_28.

Sawaya, Kali E, Leif G Olmanson, Nathan J Heinert, Patrick L Brezonik, and Marvin E Bauer. 2003. "Extending Satellite Remote Sensing to Local Scales: Land and Water Resource Monitoring Using High-Resolution Imagery." *Remote Sensing of Environment*, IKONOS Fine Spatial Resolution Land Observation, 88 (1): 144–56. https://doi.org/10.1016/j.rse.2003.04.006.

Seale, Catherine, Thomas Redfern, Paul Chatfield, Chunbo Luo, and Kari Dempsey. 2022. "Coastline Detection in Satellite Imagery: A Deep Learning Approach on New Benchmark Data." *Remote Sensing of Environment* 278 (September):113044. https://doi.org/10.1016/j.rse.2022.113044.

"Sentinel-2." 2023. In *Wikipedia*. https://en.wikipedia.org/w/index.php?title=Sentinel-2&oldid=1188518240.

"Sentinel-2 - Missions - Sentinel Online." n.d. Sentinel Online. Accessed January 29, 2024. https://copernicus.eu/missions/sentinel-2.

Sheffield, J., E. F. Wood, M. Pan, H. Beck, G. Coccia, A. Serrat-Capdevila, and K. Verbist. 2018. "Satellite Remote Sensing for Water Resources Management: Potential for Supporting Sustainable Development in Data-Poor Regions." *Water Resources Research* 54 (12): 9724–58. https://doi.org/10.1029/2017WR022437.

Sibanda, Mbulisi, Onisimo Mutanga, Vimbayi G. P. Chimonyo, Alistair D. Clulow, Cletah Shoko, Dominic Mazvimavi, Timothy Dube, and Tafadzwanashe Mabhaudhi. 2021. "Application of Drone Technologies in Surface Water Resources Monitoring and Assessment: A Systematic Review of Progress, Challenges, and Opportunities in the Global South." *Drones* 5 (3): 84. https://doi.org/10.3390/drones5030084.

Sun, Xian, Peijin Wang, Zhiyuan Yan, Wenhui Diao, Xiaonan Lu, Zhujun Yang, Yidan Zhang, et al. 2021. "Automated High-Resolution Earth Observation Image Interpretation: Outcome of the 2020 Gaofen Challenge." *IEEE Journal of Selected Topics in Applied Earth*

Observations and Remote Sensing 14:8922–40.
https://doi.org/10.1109/JSTARS.2021.3106941.

Tan, Mingxing, and Quoc Le. 2019. "EfficientNet: Rethinking Model Scaling for Convolutional Neural Networks." In *Proceedings of the 36th International Conference on Machine Learning*, 6105–14. PMLR. https://proceedings.mlr.press/v97/tan19a.html.

Taylor, Mark, and Robert Stokes. 2005. "When Is a River Not a River? Consideration of the Legal Definition of a River for Geomorphologists Practising in New South Wales, Australia." *Australian Geographer - AUST GEOGRAPHER* 36 (July):183–200. https://doi.org/10.1080/00049180500153450.

Verma, Ujjwal, Arjun Chauhan, Manohara Pai M.m., and Radhika Pai. 2021. "DeepRivWidth : Deep Learning Based Semantic Segmentation Approach for River Identification and Width Measurement in SAR Images of Coastal Karnataka." *Computers & Geosciences* 154 (September):104805. https://doi.org/10.1016/j.cageo.2021.104805.

Vickers, Hannah, Eirik Malnes, and Kjell-Arild Høgda. 2019. "Long-Term Water Surface Area Monitoring and Derived Water Level Using Synthetic Aperture Radar (SAR) at Altevatn, a Medium-Sized Arctic Lake." *Remote Sensing* 11 (23): 2780. https://doi.org/10.3390/rs11232780.

Vörösmarty, C. J., P. B. McIntyre, M. O. Gessner, D. Dudgeon, A. Prusevich, P. Green, S. Glidden, et al. 2010. "Global Threats to Human Water Security and River Biodiversity." *Nature* 467 (7315): 555–61. https://doi.org/10.1038/nature09440.

"Water-Body Segmentation | UNet Model." n.d. Accessed April 18, 2024. https://kaggle.com/code/utkarshsaxenadn/water-body-segmentation-unet-model.

Weng, Xi, Yan Yan, Genshun Dong, Chang Shu, Biao Wang, Hanzi Wang, and Ji Zhang. 2022. "Deep Multi-Branch Aggregation Network for Real-Time Semantic Segmentation in Street Scenes." *IEEE Transactions on Intelligent Transportation Systems* 23 (10): 17224–40. https://doi.org/10.1109/TITS.2022.3150350.

Wetzel, Robert G. 2001. *Limnology: Lake and River Ecosystems*. Gulf Professional Publishing.

"What Is Qualitative Data? Types, Examples & Analysis | Fullstory." n.d. Accessed July 14, 2024. https://www.fullstory.com/qualitative-data/.

Wieland, Marc, Sandro Martinis, Ralph Kiefl, and Veronika Gstaiger. 2023. "Semantic Segmentation of Water Bodies in Very High-Resolution Satellite and Aerial Images." *Remote Sensing of Environment* 287 (March):113452. https://doi.org/10.1016/j.rse.2023.113452.

Wu, Qiusheng, Charles R. Lane, Xuecao Li, Kaiguang Zhao, Yuyu Zhou, Nicholas Clinton, Ben DeVries, Heather E. Golden, and Megan W. Lang. 2019. "Integrating LiDAR Data and Multi-Temporal Aerial Imagery to Map Wetland Inundation Dynamics Using Google Earth Engine." *Remote Sensing of Environment* 228 (July):1–13. https://doi.org/10.1016/j.rse.2019.04.015.

Wu, Qiusheng, and Lucas Prado Osco. 2023. "Samgeo: A Python Package for Segmenting Geospatial Datawith the Segment Anything Model (SAM)." *Journal of Open Source Software* 8 (89): 5663. https://doi.org/10.21105/joss.05663.

Wu, Wei, Qiangzi Li, Yuan Zhang, Xin Du, and Hongyan Wang. 2018. "Two-Step Urban Water Index (TSUWI): A New Technique for High-Resolution Mapping of Urban Surface Water." *Remote Sensing* 10 (11): 1704. https://doi.org/10.3390/rs10111704.

Wulder, Michael A., Jeffrey G. Masek, Warren B. Cohen, Thomas R. Loveland, and Curtis E. Woodcock. 2012. "Opening the Archive: How Free Data Has Enabled the Science and Monitoring Promise of Landsat." *Remote Sensing of Environment*, Landsat Legacy Special Issue, 122 (July):2–10. https://doi.org/10.1016/j.rse.2012.01.010.

Xie, Y., Z. Sha, and M. Yu. 2008. "Remote Sensing Imagery in Vegetation Mapping: A Review." *Journal of Plant Ecology* 1 (1): 9–23. https://doi.org/10.1093/jpe/rtm005.

Xu, Hanqiu. 2006. "Modification of Normalised Difference Water Index (NDWI) to Enhance Open Water Features in Remotely Sensed Imagery." *International Journal of Remote Sensing* 27 (14): 3025–33. https://doi.org/10.1080/01431160600589179.

Yao, Fangfang, Chao Wang, Di Dong, Jiancheng Luo, Zhanfeng Shen, and Kehan Yang. 2015. "High-Resolution Mapping of Urban Surface Water Using ZY-3 Multi-Spectral Imagery." *Remote Sensing* 7 (9): 12336–55. https://doi.org/10.3390/rs70912336.

Yu, Yongtao, Yuting Yao, Haiyan Guan, Dilong Li, Zuojun Liu, Lanfang Wang, Changhui Yu, Shaozhang Xiao, Wenhao Wang, and Lv Chang. 2021. "A Self-Attention Capsule Feature Pyramid Network for Water Body Extraction from Remote Sensing Imagery." *International Journal of Remote Sensing* 42 (5): 1801–22. https://doi.org/10.1080/01431161.2020.1842544.

Yuan, Kunhao, Xu Zhuang, Gerald Schaefer, Jianxin Feng, Lin Guan, and Hui Fang. 2021. "Deep-Learning-Based Multispectral Satellite Image Segmentation for Water Body Detection." *IEEE Journal of Selected Topics in Applied Earth Observations and Remote Sensing* 14:7422–34. https://doi.org/10.1109/JSTARS.2021.3098678.

Yue, Xiangyu, Yang Zhang, Sicheng Zhao, Alberto Sangiovanni-Vincentelli, Kurt Keutzer, and Boqing Gong. 2019. "Domain Randomization and Pyramid Consistency: Simulation-to-Real Generalization Without Accessing Target Domain Data." In , 2100–2110. https://openaccess.thecvf.com/content_ICCV_2019/html/Yue_Domain_Randomization_and_Pyramid_Consistency_Simulation-to-Real_Generalization_Without_Accessing_Target_ICCV_2019_paper.html.

Zhang, Yindan, Gang Chen, Soe W. Myint, Yuyu Zhou, Geoffrey J. Hay, Jelena Vukomanovic, and Ross K. Meentemeyer. 2022. "UrbanWatch: A 1-Meter Resolution Land Cover and Land Use Database for 22 Major Cities in the United States." *Remote Sensing of Environment* 278 (September):113106. https://doi.org/10.1016/j.rse.2022.113106.

Zhao, Hengshuang, Jianping Shi, Xiaojuan Qi, Xiaogang Wang, and Jiaya Jia. 2017. "Pyramid Scene Parsing Network." In *2017 IEEE Conference on Computer Vision and Pattern Recognition (CVPR)*, 6230–39. Honolulu, HI: IEEE. https://doi.org/10.1109/CVPR.2017.660.